SCHATTEN MATRIX NORM BASED POLARIMETRIC SAR DATA REGULARIZATION. APPLICATION OVER CHAMONIX MONT-BLANC

Thu Trang Le, Abdourrahmane Atto, Emmanuel Trouvé

SCHATTEN MATRIX NORM BASED POLARIMETRIC SAR DATA REGULARIZATION. APPLICATION OVER CHAMONIX MONT-BLANC

Thu Trang LÊ[1], **Abdourrahmane M. ATTO**[1], **Emmanuel TROUVÉ**[1]

[1] *LISTIC, Université de Savoie - Polytech Annecy - Chambéry, BP 80439 - F-74944 Annecy-le-Vieux Cedex - France, {thu-trang.le/abdourrahmane.atto/emmanuel.trouve}@univ-savoie.fr*

Abstract

The paper addresses the filtering of Polarimetry Synthetic Aperture Radar (PolSAR) images. The filtering strategy is based on a regularizing cost function associated with matrix norms called the Schatten p-norms. These norms apply on matrix singular values. The proposed approach is illustrated upon scattering and coherency matrices on RADARSAT-2 PolSAR images over the Chamonix Mont-Blanc site. Several p values of Schatten p-norms are surveyed and their capabilities on filtering PolSAR images is provided in comparison with conventional strategies for filtering PolSAR data.

Keywords: PolSAR, filtering, geometric regularity.

1 Introduction

Since the launch of SAR satellites offering full polarization (ALOS, RADASAT-2 and TERRASAR-X, in L band, C band and X band respectively), the use of PolSAR imagery has been studied extensively in many fields, such as biomass and forest height estimation, snow cover mapping, glacier monitoring, damage assessment, etc.

The measurement of polarimetric radar is the complex scattering matrix, which can be expressed as:

$$S_2 = \begin{bmatrix} S_{hh} & S_{hv} \\ S_{vh} & S_{vv} \end{bmatrix} \quad (1)$$

where S_{hh}, S_{vv} are the scattering elements of co-polarization, and S_{hv}, S_{vh} are the scattering elements of cross-polarization associated with the wave transmitted and received on horizontal/vertical and vertical/horizontal plane respectively.

In monostatic and reciprocal backscattering case, S_{hv} = S_{vh}, the scattering information can be addressed in a complex vector as:

- Lexicographic scattering vector (k_{3L}):

$$k_{3L} = \begin{bmatrix} S_{hh} & \sqrt{2}S_{hv} & S_{vv} \end{bmatrix}^T \quad (2)$$

or

- Pauli scattering vector (k_{3P}):

$$k_{3P} = \frac{1}{\sqrt{2}} \begin{bmatrix} S_{hh} + S_{vv} & S_{hh} - S_{vv} & 2S_{hv} \end{bmatrix}^T \quad (3)$$

where superscript "T" refers to the matrix transpose.

Polarimetric information can also be presented by a covariance matrix (C_3) based on k_{3L} or a coherency matrix (T_3) based on k_{3P} as follow:

$$C_3 = \langle k_{3L}.k_{3L}^{*T} \rangle = \begin{bmatrix} \langle |S_{hh}|^2 \rangle & \sqrt{2}\langle S_{hh}S_{hv}^* \rangle & \langle S_{hh}S_{vv}^* \rangle \\ \sqrt{2}\langle S_{hv}S_{hh}^* \rangle & 2\langle |S_{hv}|^2 \rangle & \sqrt{2}\langle S_{hv}S_{vv}^* \rangle \\ \langle S_{vv}S_{hh}^* \rangle & \sqrt{2}\langle S_{vv}S_{hv}^* \rangle & \langle |S_{vv}|^2 \rangle \end{bmatrix} \quad (4)$$

and

$$T_3 = \langle k_{3P}.k_{3P}^{*T} \rangle = \frac{1}{2} \begin{bmatrix} \langle |S_{hh} + S_{vv}|^2 \rangle & \langle (S_{hh} + S_{vv})(S_{hh} - S_{vv})^* \rangle & 2\langle (S_{hh} + S_{vv})S_{hv}^* \rangle \\ \langle (S_{hh} - S_{vv})(S_{hh} + S_{vv})^* \rangle & \langle |S_{hh} - S_{vv}|^2 \rangle & 2\langle (S_{hh} - S_{vv})S_{hv}^* \rangle \\ 2\langle S_{hv}(S_{hh} + S_{vv})^* \rangle & 2\langle S_{hv}(S_{hh} - S_{vv})^* \rangle & 4\langle |S_{hv}|^2 \rangle \end{bmatrix} \quad (5)$$

where superscript " $*$ " indicates the complex conjugate, and $\langle \cdots \rangle$ denotes mathematical expectation usually estimated by temporal or spatial averaging.

The intrinsic difficulty on exploiting PolSAR data is the so-called speckle noise involved in coherent acquisition systems. Speckle reduction techniques are often required as a preprocessing step in order to improve the accuracy of image segmentation, classification, edge extraction... There are many approaches in speckle filtering for PolSAR data in literature. Novak and Burl [1] proposed the polarimetric whitening filter (PWF), which optimally combines the elements of the scattering matrix and produces a single scalar intensity image in which speckle is reduced but the polarization information is lost. Lee et al. [2] used the multiplicative speckle model and minimized the mean square error to filter the diagonal terms of the covariance matrix, which are real and represent the channel powers. Lopes and Sery [3] applied PWF for multilook complex data (MPWF) related to the texture variation using a product model for

texture and speckle noise. Vasile et al. [4] proposed an adaptive filter for coherency matrix of polarimetric or interferometric SAR data using intensity information to grow the adaptive neighborhood. To preserve the dominant scattering mechanism of each pixel, Lee et al. [5] proposed an approach that includes in the average only the pixels in the same dominant scattering category.

The two main directions for speckle filtering PolSAR data are either the selection of adaptive windows/neighborhoods or the choice of the estimator such as complex multi-looking (ML), locally linear minimum mean square error (LLMMSE), etc. In [6], authors introduced an original cost function based on l^p norms for multivariate data filtering. In this paper, we address the extension of this cost function when considering the Schatten representation of multi-channel complex PolSAR matrices. We investigate several PolSAR data characterizations issued from standard PolSAR matrix decompositions (ex: S_2, C_3, T_3,etc.). We consider a PolSAR image $\mathcal{I}$, where each pixel is characterized by a matrix. This considered matrix is still corrupted by speckle noise. Therefore we wish to replace this matrix by a matrix $\mathcal{M}$ which minimises a cost function defined as the *norm* of the difference between matrix $\mathcal{M}$ and the observed PolSAR matrices (error norm). There exist many matrix norms. Among these norms, we consider the *Schatten p-norms* which relates to the sum of the singular values of the difference matrix in our regularization cost function. The filtering strategy then consists in selecting the best matrix $\mathcal{M}$ that minimizes the above cost function from neighborhood consideration.

2 Schatten p-norm based filtering

Let us consider the following quantity:

$$\|x\|_p = \left(\sum_{i=1}^{n} |x_i|^p \right)^{\frac{1}{p}}. \tag{6}$$

This quantity defines the standard ℓ^p

- (a) norm when $p \geqslant 1$,
- (b) quasi-norm when $0 < p < 1$ and
- (c) pseudo-norm when $p = 0$.

For the sake of simplicity, we will use the terminology "norm" for the general case $p \geqslant 0$.

Since PolSAR data are matrix based images, we consider matrix norms which makes possible compact representation of the information contained in a given matrix. The following section provides these norms.

2.1 Schatten p-norms

Let $\mathcal{A}$ be an $m \times n$ matrix with the singular value decomposition (SVD) $\mathcal{A} = U\Sigma V^*$, where U and V are, respectively, an $m \times m$ and an $n \times n$ real or complex unitary matrix, and Σ is an $m \times n$ diagonal matrix with non-negative real numbers on the diagonal. The Schatten norm of order p of $\mathcal{A}$ is the ℓ^p norm of the vector of singular values of $\mathcal{A}$. This norm is:

$$\|\mathcal{A}\|_p = \left(\sum_{k=1}^{\min(m,n)} \sigma_k^p(\mathcal{A}) \right)^{\frac{1}{p}} \tag{7}$$

where σ_k is the k^{th} singular value of $\mathcal{A}$ (that is the (k,k) entry of Σ) [7].

In the rest of the paper, we will focus on 3 particular matrix norms among the family of Schatten p-norms:

- The Schatten 1-norm which is also known as the nuclear (or trace) norm.
- The Frobenius norm corresponding to the Schatten 2-norm.
- The Schatten 0.5-norm.

It is worth noticing that the singular values of a matrix are known to have a parsimony property: most energy of the matrix is concentrated on the largest singular values. In this respect, the filtering strategy discussed below is expected to be more robust than when using a standard entrywise matrix norm.

2.2 Regularization with boxcar neighborhoods and the least Schatten p error norms

Let $\mathcal{I}_{h,\ell}$ be the element located at the (h,l) pixel of image $\mathcal{I}$ and

$$\mathcal{I}[h,\ell,r] = \{\mathcal{I}_{h+i,l+j}\}_{-r\leqslant i\leqslant r,-r\leqslant j\leqslant r} \tag{8}$$

be the central pixel of a $(2r+1)\times(2r+1)$ analysis window. This window determines the boxcar neighborhood of $\mathcal{I}_{h,\ell}$ concerned by the local optimization.

The cost function $f_p(\mathcal{M}, \mathcal{I}[h,\ell,r])$ is defined by

$$f_p(\mathcal{M}, \mathcal{I}[h,\ell,r]) = \sum_{\substack{i=-r \\ j=-r}}^{r} \left[\sum_{k=1}^{Q} \sigma_k^p(\mathcal{I}_{h+i,l+j} - \mathcal{M}) \right]^{\frac{1}{p}} \tag{9}$$

where $Q = \min(m,n)$.

This function represents the Schatten p error norms of estimating $\mathcal{I}[h,\ell,r]$ by a constant value $\mathcal{M}$. In practice, we apply the above pixelwise cost function on pixel neighborhoods and seek for the matrix $\hat{\mathcal{I}}_{h,\ell}$ that minimizes the sum of pixelwise cost functions, the pixel under consideration pertaining to the pixel neighborhood $\mathcal{I}[h,\ell,r]$. The matrix $\hat{\mathcal{I}}_{h,\ell}$ is denoted by following:

$$\hat{\mathcal{I}}_{h,\ell} = \arg_{\mathcal{M}\in\mathcal{I}[h,\ell,r]} \min f_p(\mathcal{M}, \mathcal{I}[h,\ell,r]) \tag{10}$$

The image $\hat{\mathcal{I}}$ is the filtered image of the optimal values that minimize estimation errors.

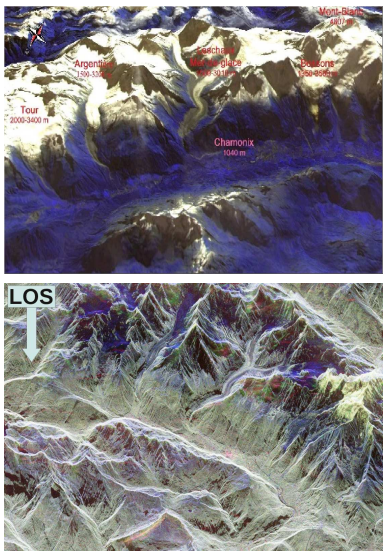

(a)

(b)

Figure 1: *Chamonix Mont-Blanc test-site. (a) Optical image warped to a DEM (b) RADARSAT2 descending image on 06/22/2009 (Pauli basis, R:HH-VV, G:2HV, B:HH+VV)*

3 Experimental results

The proposed approach is illustrated on a RADARSAT-2 ascending, quad-pol SAR image acquired on 12/24/2009. It covers a high mountain area over Chamonix Mont-Blanc which includes Alpine glaciers as Argentière and Mer de Glace - Leschaux. The test image is the sub-image over Argentière glacier. The study area is a heterogeneous area with mountainous terrain, which are mainly glacier, snow, rock mixture and some villages located sparsely. The considered matrices are scattering matrix (S_2) formed from the HH, HV and VV channels and the coherency matrix (T_3) formed from the Pauli basis.

3.1 The effect of p values to Schatten p-norm based filter

The norms which have been introduced in Section 2, provide vector spaces and their linear operators with measures of size, length and distance. They thus are widely applicable beside customary methods that we often use.

As the case of l^p norm, the Schatten p-norm based filter also depends on p values. In this section, we apply the proposed filter to the matrix S_2 and T_3 with $p = 0.5$; $p = 1$ and $p = 2$ using a sliding window of 3x3 pixels. The results obtained over the Argentière glacier image are illustrated in Fig. 6 and Fig. 7 with zoom on textured and homogeneous areas in Fig. 2; 3 for S_2 matrix and Fig. 4; 5 for T_3 matrix.

The results in Fig. 4d; 5d and 7d show that $p = 0.5$ is not an appropriate value for this filter when applied on T_3 matrix.

Fig. 2b,c and Fig. 4b,c indicate that in the case $p \geqslant 1$, the structure information is preserved quite well with sharp

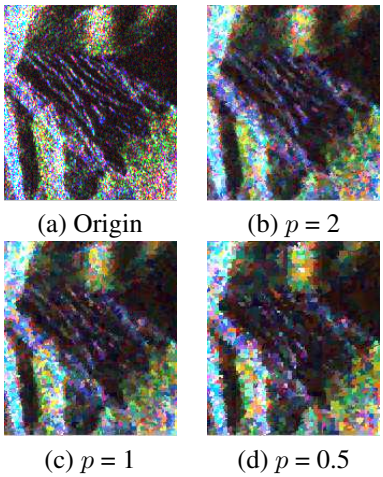

(a) Origin (b) $p = 2$ (c) $p = 1$ (d) $p = 0.5$

Figure 2: *Zoom of filtering scattering matrix S_2 using different values of p on structure area.*

(a) Origin (b) $p = 2$ (c) $p = 1$ (d) $p = 0.5$

Figure 3: *Zoom of filtering scattering matrix S_2 using different values of p on homogeneous area.*

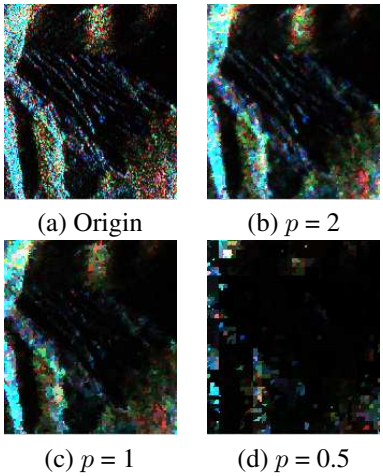

(a) Origin (b) $p = 2$ (c) $p = 1$ (d) $p = 0.5$

Figure 4: *Zoom of filtering coherency matrix T_3 using different values of p on structure area.*

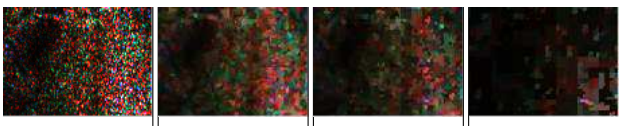

(a) Origin (b) $p = 2$ (c) $p = 1$ (d) $p = 0.5$

Figure 5: *Zoom of filtering coherency matrix T_3 using different values of p on homogeneous area.*

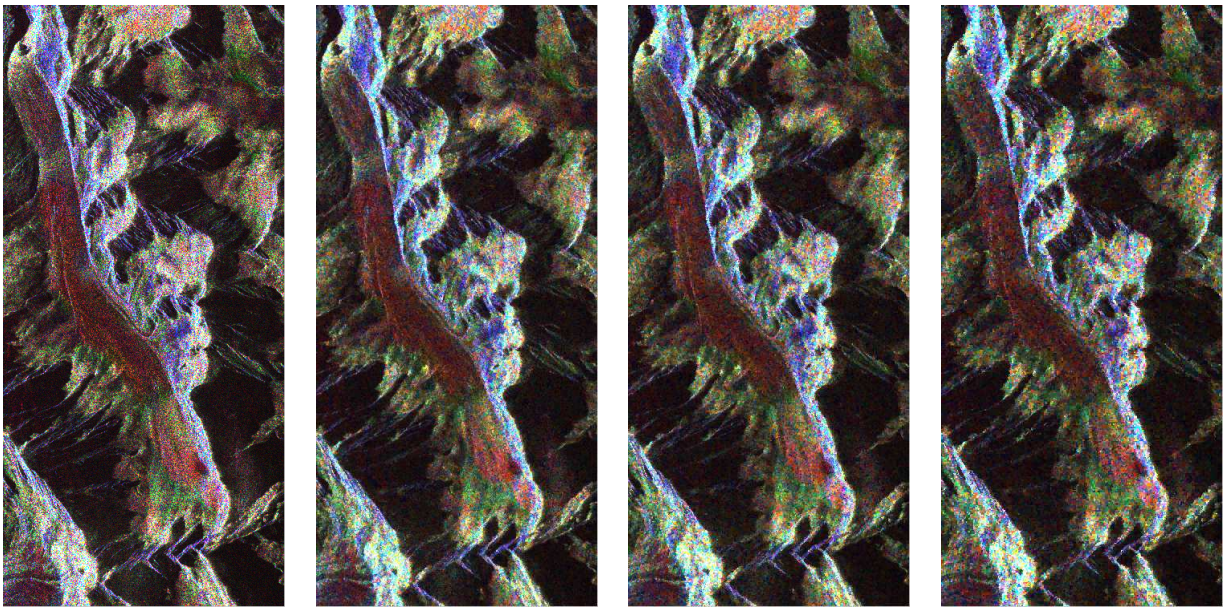

(a) Origin (b) $p = 2$ (c) $p = 1$ (d) $p = 0.5$

Figure 6: *Filtering scattering matrix S_2 using different values of p.*

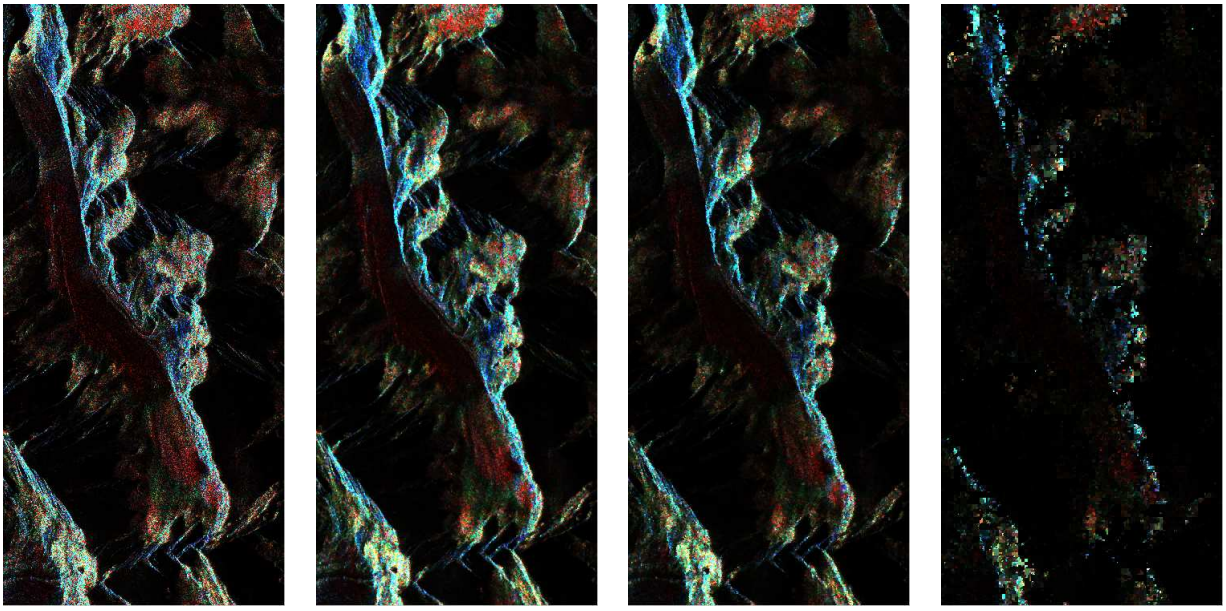

(a) Origin (b) $p = 2$ (c) $p = 1$ (d) $p = 0.5$

Figure 7: *Filtering coherency matrix T_3 using different values of p.*

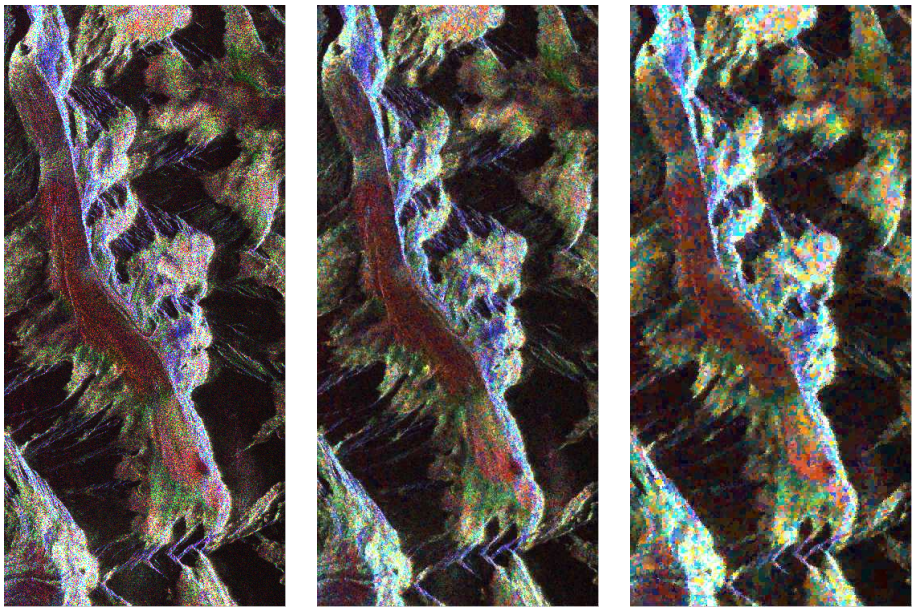

(a) Origin (b) wz = 3x3 (c) wz = 5x5

Figure 8: *Filtering scattering matrix S_2 using different window size.*

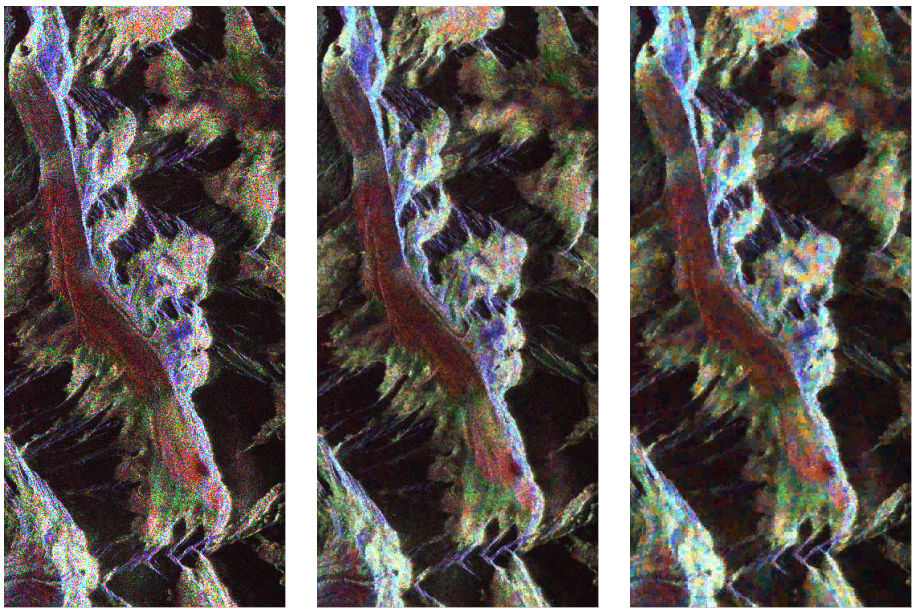

(a) (b) (c)

Figure 9: *Filtering scattering matrix S_2 with the fusion of several "p" results. (a) Original S_2 image; (b) and (c) are the filtered images with the fusion between original image, filtered images p = 0.5; p = 1; p = 2 with window size = 3x3 pixels and 5x5 pixels, respectively*

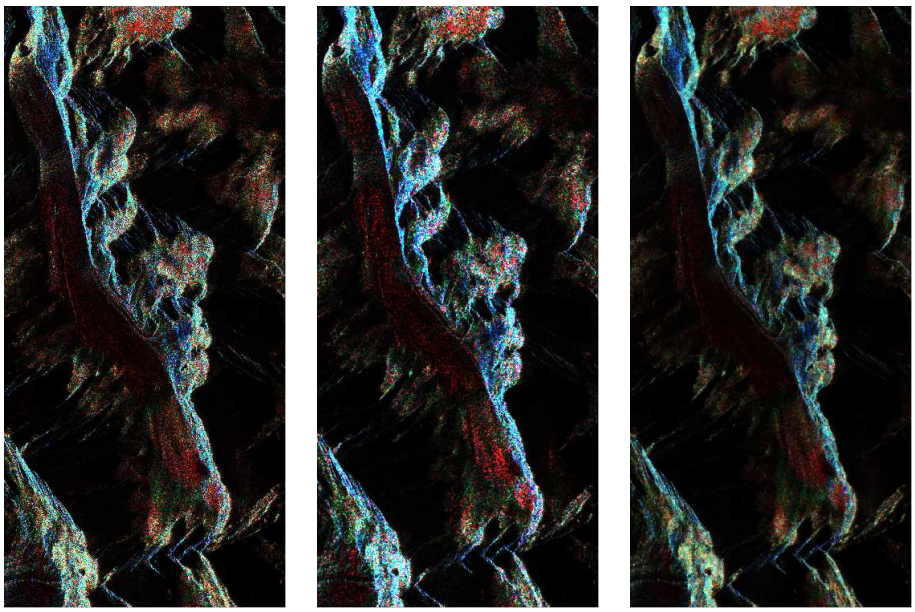

(a) (b) (c)

Figure 10: *Comparision of filtering coherency matrix T_3 between Schatten p-norm based filter and IDAN filter. (a) Original T_3 image; (b) IDAN filtered image; (c) Schatten p-norm based filtered image with the fusion between original image, filtered images p = 0.5; p = 1; p = 2 with window size = 3x3 pixels*

edges. On Fig. 3b,c and Fig. 5b,c, homogeneous area is smoother. The filtered image is smoother but not blurred while the speckle is significantly reduced.

3.2 The effect of window size to Schatten p-norm based filter

Another parameter which can impact to the efficiency of the filter is the size of analysis window. There are a number of studies about this issue in literature. In this paper, we survey the filtering strategies with window size of 3x3 and 5x5 pixels.

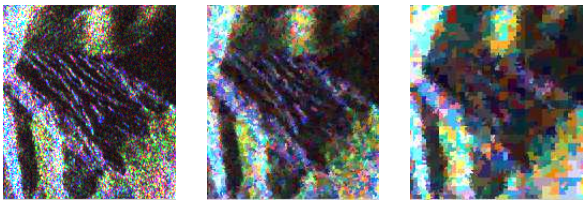

(a) Origin (b) wz = 3x3 (c) wz = 5x5

Figure 11: *Zoom of filtering scattering matrix S_2 using different window size.*

On the S_2 matrix, the results of this filter with the window size = 5x5 pixels looks like a kind of segmentation with the patch effect, but the thin structure information is lost. With the window size = 3x3 pixels, the filter operates better. To compare the operation of the filter on S_2 and T_3, it works better on S_2.

3.3 The fusion of different Schatten p-norms based filtered images with respect to p values

On the complex test-site, the filtering results should preserve structures after speckle removal. The proposed filter concerns a test-site involving both non-smooth structure and smooth areas. A given Schatten p-norm can have desirable properties or limitations depending on the area we focused on. Thus, in order to be more adaptive to the specific site, we consider combining the results of different Schatten p-norms and the original image. The fusion simply consists the sum of the intensities used to obtain the color images. Fig 9, 10, 12, 13, 14 and 15, indicate that the fusion strategy leads a better performance of filtering that the structure features of the original image are preserved and the speckle is also removed significantly. A visual comparison with IDAN filter [4] in Fig. 10, 14 and 15 show that the fusion of the Schatten p-norm based filtered images seems to be more speckle removed, clearer with more small preserved details than IDAN filtered image.

4 Conclusions and perspectives

The original method presented in this paper provided several early results which have demonstrated its potential in filtering PolSAR data.

- This filter can operate with many kind of data format of PolSAR data.

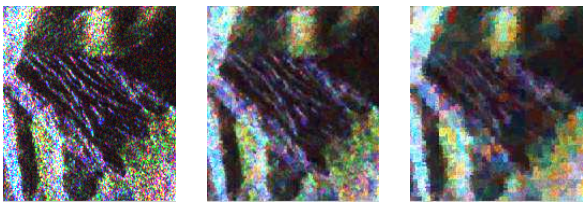

(a) (b) (c)

Figure 12: *Zoom of filtering scattering matrix S_2 with the fusion of several "p" results on structure area. (a) Original S_2 image; (b) and (c) are the filtered images with the fusion between original image, filtered images p = 0.5; p = 1; p = 2 with window size = 3x3 and 5x5 pixels, respectively*

(a) (b) (c)

Figure 13: *Zoom of filtering scattering matrix S_2 with the fusion of several "p" results on homogeneous area. (a) Original S_2 image; (b) and (c) are the filtered images with the fusion between original image, filtered images p = 0.5; p = 1; p = 2 with window size = 3x3 and 5x5 pixels, respectively*

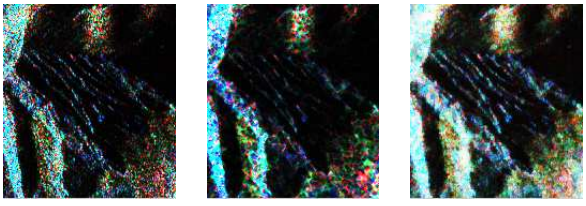

(a) (b) (c)

Figure 14: *Zoom of comparision of filtering coherency matrix T_3 between Schatten p-norm based filter and IDAN filter on structure area. (a) Original T_3 image; (b) IDAN filtered image; (c) Schatten p-norm based filtered image with the fusion between original image, filtered images p = 0.5; p = 1; p = 2 with window size = 3x3 pixels*

(a) (b) (c)

Figure 15: *Zoom of comparision of filtering coherency matrix T_3 between Schatten p-norm based filter and IDAN filter on homogeneous area. (a) Original T_3 image; (b) IDAN filtered image; (c) Schatten p-norm based filtered image with the fusion between original image, filtered images p = 0.5; p = 1; p = 2 with window size = 3x3 pixels*

- Choosing different values of p brings us different strategies that are optimal in the Schatten p error norm sense for filtering PolSAR data.
- If we choose an appropriate p value, we can take the advantage of Schatten p-norms (mentioned in Section 2.1) to increase sparsity.

The further works to develop this method may concern:

- implementing performance assessment for filtered images
- looking for initial transform to exploit sparsity
- studying fusion strategies to reach a better performance
- applying the proposed method in different decomposition/coding to exploit polarization information of PolSAR data.

References

[1] Novak, L.M. & Burl, M.C. (1990). Optimal speckle reduction in polarimetric SAR imagery. *IEEE Trans. Aerosp. Electron. Syst.* 26(2), 293-350

[2] Lee, J.S., Grunes, M.R. & Mango, S.A. (1991). Speckle reduction in multipolarization and multifrequency SAR imagery. *IEEE Trans. Geosi. Remote Sensing.* 29(4), 535-544

[3] Lopes, A. & Sery, F. (1997). Optimal speckle reduction for the product model in multilook polarimetric SAR imagery and the whishart distribution. *IEEE Trans. Geosi. Remote Sensing.* 35(3), 632-647

[4] Vasile, G., Trouve, E., Lee, J.S. & Buzuloiu, V. (2006). Intensity-driven adaptive-neighborhood technique for polarimetric and interferometric SAR parameters estimation. *IEEE Trans. Geosi. Remote Sensing.* 44(6), 1609-1621

[5] Lee, J.S., Grunes, M.R., Schuler, D.L., Pottier, E. & Ferro-Famil, L. (2006). Scattering-model-based speckle filtering of polarimetric SAR data. *IEEE Trans. Geosi. Remote Sensing.* 44(1), 176-187

[6] Atto, A.M., Mercier, G., Le, T.T. & Trouve, E. (2012). Vector and matrix LP norms in polarimetric radar filtering. *IEEE Proc. IGARSS.* 1441-1444

[7] Lefkimmiatis, S., Ward, J.P. & Unser, M. (2013). Hessian Schatten-norm regularization for linear inverse problems. *To appear in IEEE Trans. Image Processing.*